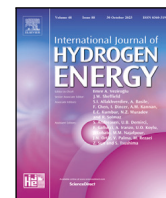




Contents lists available at ScienceDirect

International Journal of Hydrogen Energy

journal homepage: www.elsevier.com/locate/he

Hydrogen storage minimization under industrial flexibility constraints: A techno-economic analysis of off-grid green ammonia production

Zachary Tully ^{a, *}, Jennifer King ^b, Kathryn Johnson ^{c, b}

^a Advanced Energy Systems Graduate Program, Colorado School of Mines, Golden CO 80401, USA

^b National Renewable Energy Laboratory, Golden CO 80401, USA

^c Electrical Engineering Department, Colorado School of Mines, Golden CO 80401, USA

ARTICLE INFO

Keywords:

Flexible ammonia
Off-grid hybrid wind and solar generation
Hydrogen storage
Seasonal variability
Optimal year-long ammonia plant operating profile

ABSTRACT

Electrifying ammonia production using renewable energy (RE) and water electrolysis is a critical step in the worldwide transition from fossil fuels to alternative energy sources. However, the common requirement that the ammonia reactor operate at a steady production level harms the system's economic feasibility due to the large hydrogen and battery storage required to overcome RE variability. In this study, we examine the sensitivity of the plant storage capacity requirement to the flexibility of the ammonia reactor. We examine two aspects of ammonia reactor flexibility: ramping rate flexibility and the range of operation (turndown flexibility). We develop a storage dispatch and ammonia reactor scheduling optimization, which computes the minimum storage requirement given a RE generation profile and set of reactor flexibility parameters. We optimize across a sweep of flexibility parameters for two locations in the United States. We find that turndown flexibility is the most important, while ramping flexibility has little effect on the overall storage requirement. Further, we see that seasonal variability in the RE generation profile is the primary driver of high storage capacity requirement. We find that with a turndown flexibility of 60% of the ammonia plants rated capacity, which is understood to be achievable with existing ammonia reactor technology, the storage capacity was reduced by 84 % in one of the locations we examined, which resulted in a 22% decrease in the levelized cost of ammonia with pipe-based hydrogen storage.

1. Introduction

Ammonia is an essential chemical to humankind, as it is the main ingredient in fertilizers that help produce the world's food supply. Ammonia may also serve a role in the transition to renewable energy (RE) as an energy storage vector and carbon-free fuel. However, ammonia production is responsible for 1.3% of global energy sector CO₂ emissions [1], which is quite substantial for a single industry. In order to continue supporting food production and meet climate goals, the carbon intensity of ammonia production must be drastically reduced.

Ammonia is most commonly produced using the Haber–Bosch process [1,2], which combines hydrogen and nitrogen in the presence of an iron catalyst at elevated temperature and pressure to synthesize ammonia. The primary source of emissions from ammonia production is the steam methane reformation process used to supply the hydrogen feedstock to the Haber–Bosch reactor (HBR) [3]. Additional emissions come from any fossil fuel-based electricity used to extract nitrogen from the air and run the auxiliary equipment in the ammonia plant.

In their techno-economic comparison of several ammonia decarbonization pathways, Wang et al. identify RE-powered, electrolytic-hydrogen-fed Haber–Bosch to be the most promising option for decarbonizing ammonia generation in the near-future [4]. Using RE to supply the hydrogen feedstock via water electrolysis and for the plant's auxiliary energy needs, effectively eliminates fossil fuels from the plant's inputs. With no fossil fuels in the feedstocks, the plant output is low-emission green ammonia.

However, the temporal variability of wind- and solar-powered electricity and hydrogen generation poses a challenge for HBRs, which are traditionally operated at steady-state. To support a steady-state HBR, large-scale storage assets are needed to buffer the variability in the hydrogen and electricity feedstocks. This large-scale storage requirement and its associated cost is one of the major hurdles limiting the viability of RE-powered green ammonia.

If instead of operating at steady-state, the HBR is allowed to operate flexibly, then the storage requirement may be reduced, thus lowering the cost RE-powered green ammonia. However, the impacts of flexible

* Corresponding author.

E-mail addresses: tully@mines.edu, ztully@nrel.gov (Z. Tully).

<https://doi.org/10.1016/j.ijhydene.2025.02.109>

Received 22 July 2024; Received in revised form 5 February 2025; Accepted 6 February 2025

Available online 22 February 2025

0360-3199/© 2025 The Authors. Published by Elsevier Ltd on behalf of Hydrogen Energy Publications LLC. This is an open access article under the CC BY-NC-ND license (<http://creativecommons.org/licenses/by-nc-nd/4.0/>).

Nomenclature

μ	Mean feedstock generation
\bar{d}, d	Maximum, minimum end-use feedstock demand
\bar{g}	Maximum feedstock generation
\bar{M}_{H_2}	Hydrogen storage capacity
\bar{R}	End-use ramping rate limit
C_{ASU}	Air separation unit capacity
C_{Bat}	Battery capacity
C_{EL}	Electrolyzer capacity
$C_{H_2St.}$	Hydrogen storage capacity
C_{HBR}	Haber–Bosch reactor capacity
C_{SF}	Solar farm capacity
C_{WF}	Wind farm capacity
d_k	End-use feedstock demand at time k
E_k	Energy in battery storage at time k
f_R	Ramping flexibility
f_T	Turndown flexibility
g_k	Feedstock generation at time k
$M_{H_2,k}$	Hydrogen in hydrogen storage at time k
R_k	Ramping rate from hour $k - 1$ to hour k
T	Turndown ratio

HBR operation on the design, operation, and economics of the rest of the plant not well understood. In this paper, we aim to characterize the value of HBR flexibility by addressing the following research questions:

1. What is the sensitivity of storage capacity to HBR flexibility?
2. What is the sensitivity of levelized cost of ammonia (LCOA) to HBR flexibility?

In answering these questions, we hope identify relationships between the system design, operation, and economics that will inform future RE-powered flexible green ammonia systems. The remainder of this paper is organized as follows: We provide a background on relevant literature on ammonia decarbonization and flexibility analysis in Section 2. We present the flexible green ammonia system models and hydrogen storage optimization in Section 3, and the simulation and parameter sweep in Section 4. Finally, we conclude with a discussion of the impacts of flexibility and storage on the LCOA in Section 5.

2. Background

With the increasing interest in ammonia decarbonization, researchers are investigating the flexibility of the Haber–Bosch process from variety of perspectives. Using a steady-state process model, Cheema and Krewer [15,16] identify the upper and lower limits for a selection of process variables including temperatures, pressures, and stoichiometric ratios throughout the system. They define flexibility limits by varying process variables until the reaction is no longer autothermal and requires additional heating or cooling. The work in [16] is expanded by Fahr et al. [17], who optimized the design of the ammonia synthesis loop for enhanced flexibility, finding that modifying the design of certain HBR components, enables greater flexibility in the process variables than in [16].

Building on the steady-state flexibility analysis, the authors of [18–20] develop dynamic models of ammonia reactors with feedstocks generated by variable RE. Deng et al. [18] and Sun et al. [20] model the reactor startup dynamics during periods of intermittency. Rosbo et al. [19] develop a controller to manage time-varying reactor inputs while maintaining the stability of the ammonia synthesis loop near unstable operating points close to the flexibility limits. While [18–

20] develop excellent models and controllers for exploring the capabilities of flexible ammonia reactor operation, they only investigate operational effects without in-depth analysis of system design or cost.

Techno-economic analyses expanding on the results from these purely technical studies provide a framework to identify the impacts of HBR flexibility. A list of techno-economic investigations relevant to this study are presented in Table 1. Among the studies in Table 1, the RE resource characteristics and the degree of HBR flexibility are found to be significant drivers of LCOA.

Armijo et al. [8] find wind and solar variability to be the root cause that drives the need for large-scale hydrogen storage and HBR flexibility and conclude that leveraging hybrid wind/solar generation to reduce variability can improve costs. Smith et al. [13] also examine generation variability using artificial RE resource signals constructed of sine waves with varying period to imitate RE variability on different timescales. The authors of [13] find seasonal variability to be the main factor behind hydrogen storage requirement and a significant driver of LCOA. Nayak-Luke et al. [11] and Fasihi et al. [3] both perform sweeps comparing several locations around the world. Both studies show that the sites with low variability and high wind and solar capacity factors yield lower LCOA.

A number of the studies in Table 1 examine ramping rate flexibility and/or turndown flexibility in their analyses and several authors provide similar conclusions. Armijo et al. [8], Campion et al. [9], Nayak-Luke et al. [21], and Wang et al. [14] consider both ramping and turndown flexibility and all find that turndown flexibility is far more impactful on the storage requirement and LCOA than the ramping rate flexibility. Campion et al. [9], Salmon et al. [12], both analyze a number of distinct turndown flexibility scenarios and find that increased turndown flexibility allows the HBR to more closely follow the RE generation reducing storage requirement and improving LCOA. However both studies find diminishing marginal benefits for high levels of turndown flexibility [9,12]. Campion et al. find that a turndown limit of 40%–60% of the HBR rated capacity provides significant costs savings but that increasing HBR flexibility further yields only marginal improvements [9]. Salmon et al. find the cost savings drop off beyond a turndown limit of 60% of HBR rated capacity [12]. The point of diminishing returns identified in [9,12] is an important factor in understanding the value of HBR flexibility, however both studies use relatively coarse flexibility sweeps so it is difficult to characterize this effect.

Advancements in hydrogen storage technology hold potential for achieving additional future cost reductions. Hydrogen can be stored in various forms, including as a compressed gas, through chemical processes, and via adsorption. While adsorption and chemical storage methods offer certain advantages over compressed gas storage such as improved efficiency and potentially lower cost, these options not technologically mature and are therefore not viable alternatives in the short term [22]. For compressed gas hydrogen storage, the available options include pipe or tank-based storage, and cavern-based storage utilizing either steel-lined rock caverns or salt caverns [23]. Among these options, salt cavern storage is the most economically attractive [22,23]; however, its applicability is geographically constrained limiting its broader implementation. Among the literature in Table 1, some authors consider salt cavern storage [3,8], but the majority assume hydrogen storage in pipe- or tank-based systems.

Among these works, there is consensus that increasing HBR flexibility reduces the storage requirement, improves LCOA, and may be critical for achieving cost-competitive RE-powered green ammonia. However, the sensitivity of system design and economics to HBR flexibility is not well-defined in the literature. The main contribution of our study is that we map out these sensitivities in greater detail than existing research so that RE-powered green ammonia systems may gain the most value from HBR flexibility.

Table 1

Summary of relevant literature on RE-powered green ammonia case studies. Despite implementation differences, many of these studies find a LCOA of 500 USD/t or lower to be attainable although some authors find significantly higher values. Studies in the “Flexible” category consider HBR flexibility in their analyses and are used to inform the techno-economic parameters in this work.

Ref.	Grid	Storage	NH ₃ capacity (t/year)	LCOA (USD/t)	Location(s)	Flexibility extent
Inflexible						
[3]	no	battery, hydrogen (pipe and cavern)	400 000	465	World	–
[5]	yes	battery, hydrogen (pipe)	443 475	580	Iran	–
[4]	yes	battery, hydrogen (pipe)	36 500	460	–	–
[6]	yes	battery, hydrogen (pipe)	50 000	677	–	–
[7]	no	battery, hydrogen (pipe), thermal	671 600	450	U.A.E.	–
Flexible						
[8]	yes	battery, hydrogen (pipe and cavern)	35 000	487	Chile, Argentina	ramping: 20%/h turndown: 60%
[9]	yes	battery, hydrogen (pipe)	499 320	803	Chile, Denmark, Australia	ramping: 20%/h turndown: 40%
[10]	no	battery, hydrogen (pipe), thermal	1460	774	Morocco	ramping: 20%/h
[11]	no	battery, hydrogen (pipe)	–	660	World	ramping: 100%/h
[12]	no	battery, hydrogen (pipe)	1 533 000	540	–	turndown: 20%
[13]	no	battery, hydrogen (pipe)	36 500	800	UK, Spain	turndown: 40%
[14]	no	battery, hydrogen (pipe)	–	483	Australia	ramping: 20%/h turndown 40%
This study	no	battery, hydrogen (pipe and cavern)	245 000	508	United States	ramping: 20%/h turndown: 60%

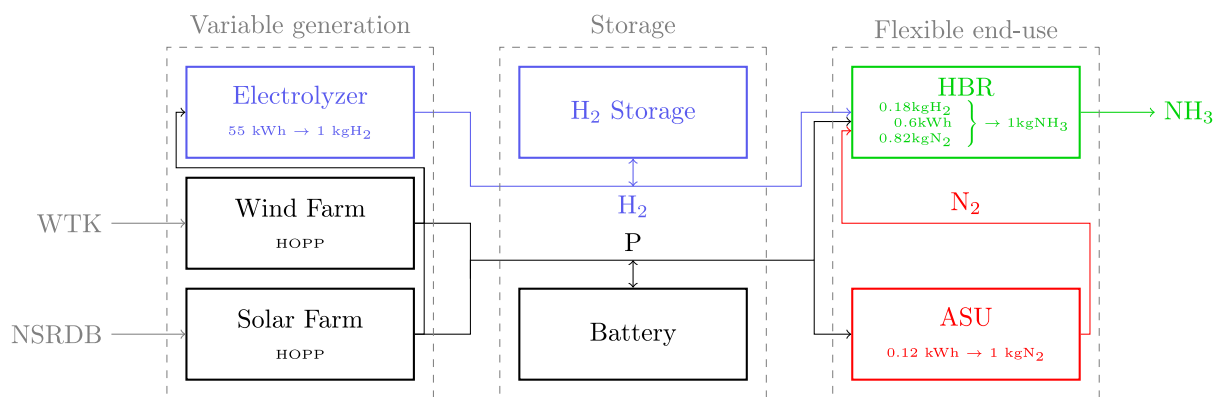


Fig. 1. Block diagram of the RE-powered off-grid green ammonia system in this study. Arrows in black represent electrical power transfer, blue arrows represent hydrogen flow, red arrows represent nitrogen flow, and green arrows represent ammonia output. The individual components are grouped into generation, storage, and end-use subsystems based on their role in generating, storing, or consuming the HBR feedstocks. Wind resource data is from the NREL Wind Toolkit [24], and solar resource data from the NREL National Solar Radiation Database [25].

3. Materials and methods

In this work, we model flexible ammonia synthesis via the Haber–Bosch process, which is described by the chemical reaction in Eq. (1) [15].

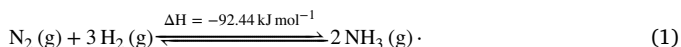


Fig. 1 shows the full green ammonia system with pathways from wind and solar resources to the hydrogen, nitrogen, and power feedstock into the ammonia plant. The components are grouped into three subsystems based on their role in providing the feedstocks to the HBR. The variable generation subsystem contains the electrolyzer, wind farm, and solar farm, which produce the time-varying hydrogen and electrical feedstocks. The storage subsystem has hydrogen storage and a small battery to support the relatively modest power requirements of the end-use components. The flexible end-use subsystem contains the air separation unit (ASU) and HBR.

The goal of this work is to identify the value of HBR flexibility by finding the optimal sizing of the storage and end-use subsystems for a given generation scenario and flexibility level. The diagram in

Fig. 2 shows the order of calculations used in this analysis. Section 3.1 presents variable generation subsystem model used in Steps 1 and 2 of Fig. 2, Section 3.2 describes the end-use subsystem model, and Section 3.3 explains the storage subsystem model. Section 3.2.2 describes how the end-use subsystem is sized based on the generation profile and flexibility level in Step 3 of Fig. 2 and Section 3.4 explains how the minimum storage capacity is computed in Step 4. The LCOA calculation in Step 5 is presented in Section 4.4.

3.1. Variable generation subsystem model

In our analysis, wind and solar power generation are modeled using the NREL Hybrid Optimization and Performance Platform (HOPP) software [27], which runs a year-long simulation at hourly resolution leveraging the NREL wind toolkit (WTK) [24] and National Solar Radiation Database (NSRDB) [25] for resource data. HOPP is used to compute the hydrogen and power generation timeseries in Step 2 of Fig. 2. We use proton exchange membrane (PEM) electrolyzers in this work because their quick dynamics, on the order of seconds, makes them well-suited to follow variable renewable power despite a slightly higher cost than alternatives. The electrolyzer is modeled as a constant

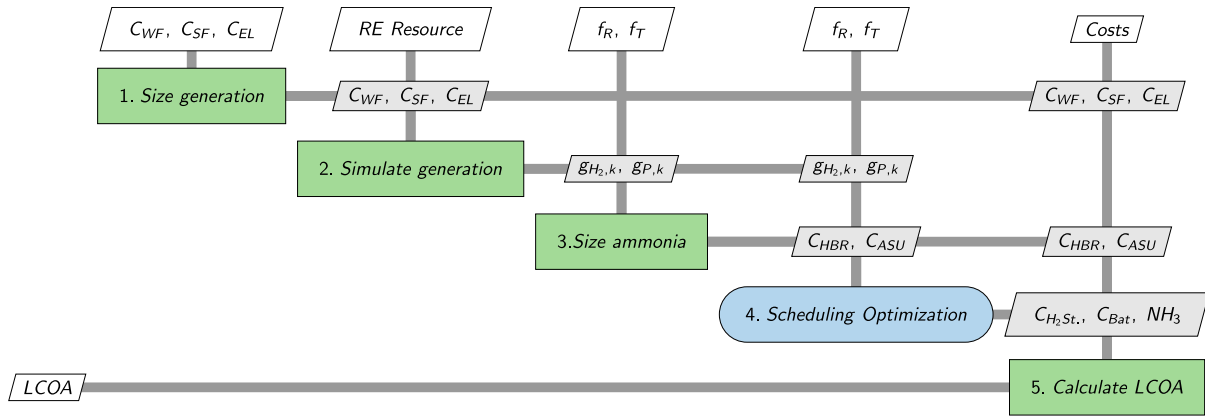


Fig. 2. XDSM diagram [26] showing the order of calculations in this research. The parameters coming into the top of each step represent the required inputs to that step and variables coming out of the right represent the outputs from that step. In Step 1, the capacities of the generation subsystem components C_{WF} , C_{SF} , C_{EL} are defined. In Step 2., the hydrogen $g_{H_2,k}$ and power $g_{P,k}$ generation profiles are computed using HOPP [27]. In Step 3., the capacities of the end-use subsystem components C_{HBR} , C_{ASU} are defined using the heuristic method in Section 3.2.2. In Step 4., the scheduling optimization in Section 3.4 is calculated, which yields the capacities of the storage subsystem $C_{H_2,St.}$, C_{Bat} and the total ammonia production NH_3 . In Step 5., the LCOA is calculated as described in Section 4.4.

Table 2

Rated capacities of the generation subsystem components. The system rated for 1 GW of electrical generation and the electrolyzer is rated in proportion to the electrical demands of the HBR and ASU.

Component	Capacity
Wind Farm	$C_{WF} = 500$ MW
Solar farm	$C_{SF} = 500$ MW
Electrolyzer	$C_{EL} = 933$ MW

conversion of electrical power to hydrogen with a conversion rate of 55 kWh/kgH₂ [28] and is assumed to operate proportionally to the wind and solar generation.

The green ammonia plant studied in this work is not connected to the grid, so it cannot buy or sell power. We choose to investigate off-grid power generation because it is a more restrictive case than grid-connected and expect that any benefits of flexibility in the off-grid case could also benefit the grid-connected case. Also, growing concerns regarding the insufficient buildout of transmission infrastructure to support electrification [29] provides additional motivation for investigating off-grid plants.

The wind and solar farms in this study have a combined nominal capacity of 1 GW with individual capacities of 500 MW each. The wind farm capacity C_{WF} , solar farm capacity C_{SF} , and electrolyzer capacity C_{EL} are listed in Table 2. The component capacities from Table 2 are used as the inputs to Step 1 in Fig. 2. The optimal split of wind and solar generation is highly location-dependent [30] and something we hope to explore in future research. In this work, we use equal wind and solar capacity to take advantage of complementarity while avoiding bias towards a single RE technology.

3.2. Flexible end-use subsystem model

The end-use subsystem from Fig. 1 consists of the HBR and ASU, which are assumed to operate proportionally to each other. The ASU is modeled as a constant-efficiency conversion of electricity with an efficiency of 0.119 kWh/kg N₂ [21]. The HBR is also modeled as a constant-efficiency conversion process with an energy consumption of 0.6 kWh/kg NH₃ [21]. The HBR also requires hydrogen and nitrogen feedstocks in the stoichiometric ratio from (1). We assume the HBR uses the standard Haber–Bosch process with an iron catalyst.

The Sankey diagram in Fig. 3 shows the intermediate pathways that the energy in the plant takes to produce hydrogen and nitrogen for the ammonia reactor. With the electrolyzer model from Section 3.1

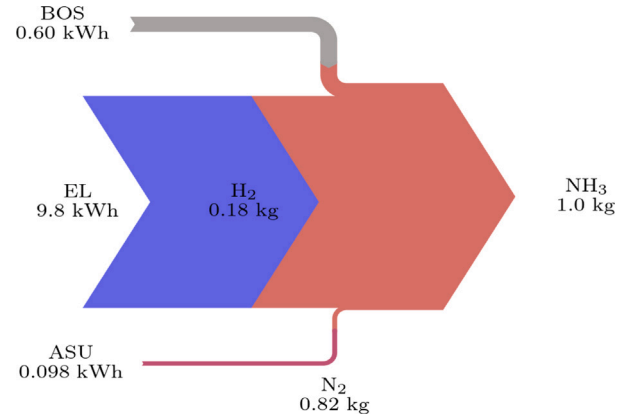


Fig. 3. Sankey diagram of the energy pathways from RE electricity to ammonia. The majority of the electricity input goes into the hydrogen feedstock with a comparatively small fraction being used for the nitrogen feedstock and balance of system components. The total conversion rate is 10.50 kWh/kg NH₃ or 37.7 GJ/t NH₃.

the total conversion efficiency of the system is 10.50 kWh/kg NH₃ or 37.7 GJ/t NH₃, which aligns with the findings of Smith et al. [31] for electrolysis-based Haber–Bosch ammonia production.

3.2.1. HBR flexibility

During simulation, the HBR operation is directly proportional to d_k , the demand for feedstocks during the k th hour of the year. The HBR operates subject to two flexibility constraints: ramping flexibility f_R , and turndown flexibility f_T . The ramping rate during the k th hour of the simulation is

$$R_k = (d_k - d_{k-1})/\Delta t, \quad (2)$$

where $\Delta t = 1$ hr is the time step. The maximum ramping rate \bar{R} imposes an upper limit on the hourly ramping rate such that $|R_k| \leq \bar{R}$, $\forall k$. The feedstock demand d_k is also constrained to an operating range: $\underline{d} \leq d_k \leq \bar{d}$, $\forall k$, where \underline{d} and \bar{d} are lower and upper limits on d_k , respectively. The turndown ratio T , is the ratio of these two limits:

$$T = \bar{d}/\underline{d}. \quad (3)$$

The HBR capacity C_{HBR} is proportional to \bar{d} , so T can be interpreted as the ratio of the minimum HBR operating point to the rated HBR operating point. For consistent notation, ramping flexibility is defined

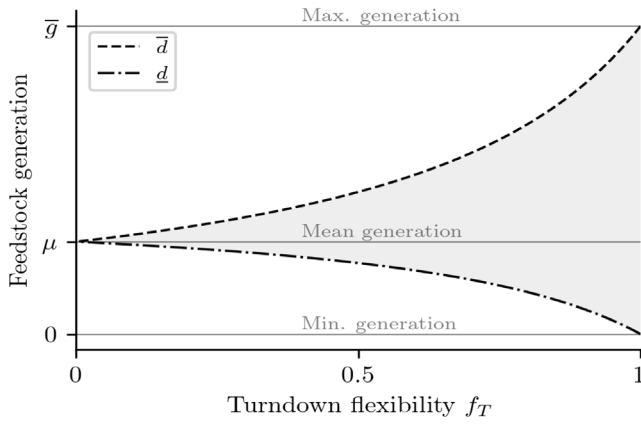


Fig. 4. Illustration of the HBR sizing as a function of f_T . The HBR is sized based on the upper demand limit \bar{d} , which is set to the mean generation μ when $f_T = 0$ and the maximum generation \bar{g} when $f_T = 1$. With higher f_T , the HBR can accommodate greater RE variability but it also becomes increasingly oversized.

as

$$f_R = \bar{R} \in [0, 1] \quad (4)$$

and turndown flexibility as

$$f_T = 1 - T \in [0, 1], \quad (5)$$

hence both parameters are more flexible the closer their value is to 1.

3.2.2. HBR sizing

The rated capacity of the HBR should be tailored to fit each flexibility case and generation scenario so that the feedstock demand is matched to the feedstock generation. If the HBR is inflexible with $f_T = 0$, then it should be rated to consume the mean feedstock generation μ during the year (i.e. $\bar{d} = \mu$) so that it can achieve the highest possible capacity factor. If instead, the HBR is fully flexible with $f_T = 1$, the it should be rated to consume the maximum feedstock generation \bar{g} during the year (i.e. $\bar{d} = \bar{g}$) so that it can follow the variable RE generation and eliminate the need for storage altogether. Between these two bounding cases, we develop a heuristic sizing method to specify \bar{d} and \underline{d} as functions of μ , \bar{g} , and f_T shown in (6) and (7) and plotted in Fig. 4.

$$\bar{d} = \frac{\mu}{1 + (\mu/\bar{g} - 1)f_T} \quad (6)$$

$$\underline{d} = \frac{\mu f_T}{1 + (\mu/\bar{g} - 1)f_T} \quad (7)$$

Eqs. (6) and (7) are designed to produce the two bounding cases described above while maintaining (3) and (5) in between. This sizing methodology is used in Step 3 of Fig. 2. Using (6) and (7) to define the HBR capacity may result in oversizing the reactor for the high flexibility cases because it must consume the highest peaks in hydrogen generation, which happen infrequently.

3.3. Storage subsystem model

The storage subsystem in Fig. 1 consists of a hydrogen storage component and battery storage component. Hydrogen storage is more cost-effective than battery storage at large scale [22] so it is preferable to convert the energy to hydrogen instead of charging a battery. The battery storage is necessary to run the ASU and auxiliary equipment in the ammonia plant but is relatively small compared to the hydrogen storage in terms of stored energy capacity.

Both the hydrogen and battery storage are modeled as integrators where the storage states, E (battery) and M_{H_2} (hydrogen storage), are

equal to the discrete integration of the charging/discharging over all preceding time steps. The storage states are described by

$$E_k = \sum_{i=0}^k (g_{P,k} - d_{P,k}) \Delta t \quad \forall k \quad (8)$$

$$M_{H_2,k} = \sum_{i=0}^k (g_{H_2,k} - d_{H_2,k}) \Delta t \quad \forall k. \quad (9)$$

The generation g_k and demand d_k at time k are further differentiated by the subscripts P and H_2 for power and hydrogen, respectively. The hydrogen storage and battery are charged and discharged proportionally to each other to maintain the correct stoichiometric ratios of ammonia plant feedstocks.

3.4. Scheduling optimization

The hydrogen storage and battery are characterized by their energy capacities and maximum charge/discharge rates, both of which are computed in the scheduling optimization in (10). The purpose of the storage subsystem is to support the HBR by absorbing the inevitable discrepancies between the generation and consumption of HBR feedstocks. We optimize the dispatch of the end-use and storage subsystems in (10) for a representative year to find the end-use operating schedule, that minimizes the hydrogen storage capacity for a given generation profile.

$$\min_{d_k, M_{H_2,k}} \bar{M}_{H_2} \quad (10a)$$

$$s.t. \quad \bar{M}_{H_2} \geq M_{H_2,k} \quad \forall k \quad (10b)$$

$$M_{H_2,k} = M_{H_2,k-1} + g_{H_2,k} - d_{H_2,k} \quad \forall k \quad (10c)$$

$$\underline{d} \leq d_{H_2,k} \leq \bar{d} \quad \forall k \quad (10d)$$

$$|d_{H_2,k} - d_{H_2,k-1}| / \Delta t \leq \bar{R} \quad \forall k \quad (10e)$$

$$M_{H_2,k} \geq 0 \quad \forall k \quad (10f)$$

$$M_{H_2,0} = M_{H_2,8760} \quad (10g)$$

The hydrogen demand d_k and hydrogen storage state $M_{H_2,k}$ are chosen at each hour-long interval k of the year to minimize the storage capacity, which is equal to the maximum hydrogen storage state \bar{M}_{H_2} during the year. The hydrogen storage charges and discharges to absorb the hourly difference between hydrogen generation g_k and HBR feedstock demand d_k according to (10c), which reflects the storage model in (9). The turndown flexibility is enforced through (10d) using the demand constraints from (6) and (7), and the ramping flexibility is enforced through (10e). Constraint (10g) ensures that the storage charging and discharging is balanced throughout the year. The optimization problem is implemented in Python and solved using the SciPy optimization package [32].

Since we are solving for a representative year in the plant's life, the exact starting date for the dispatch schedule can be arbitrarily chosen without affecting the results. Accordingly, the storage state may be non-zero at the start of the dispatch schedule. Constraint (10g) ensures that the storage subsystem can only shift feedstock generation within the representative year and prohibits inter-year generation shifting. Constraint (10g) is a necessary condition to use the results of (10) as a representative average throughout the plant life.

With the solution to (10), the hydrogen storage capacity $C_{H_2,st.}$ and battery storage capacity C_{Bat} are set based on the maximum hydrogen storage state \bar{M}_{H_2} and the ammonia production is computed from the end-use subsystem dispatch schedule, which is shown by Step 4 of Fig. 2.

Together, the first four steps in Fig. 2 provide a methodology to calculate the optimal plant design for a given HBR flexibility, which begins to answer our first research question posed in Section 1. Through this methodology, it is apparent that increasing flexibility reduces

Table 3
Ramping and turndown flexibility attainable with traditional Haber–Bosch from the literature. We use the values from [1] to represent the best available technology case.

Source	[33]	[8]	[15]	[17]	[19]	[1]
f_R	0.04	0.20	–	–	0.60	0.20
f_T	0.25	0.40	0.66	0.87	0.80	0.40

the amount of storage needed, which in turn reduces the LCOA. To answer the research questions, and characterize the sensitivity of both the storage capacity and the LCOA to HBR flexibility, we apply our methodology in the parameter sweep described in Section 4.3.

4. Results

In this section, we present the parameter sweep used to identify the sensitivity of storage capacity and LCOA to HBR flexibility. The flexibility attainable with current technology is discussed in Section 4.1, the locations investigated in the sweep are described in Section 4.2, the results of the sweep are given in Section 4.3, and the LCOA cost equations are described in Section 4.4.

4.1. HBR flexibility with current technology

To contextualize the results, we add a few additional remarks from the literature. There is little consensus in literature on what level of flexibility is achievable with today’s Haber–Bosch technology. With different analysis methods — physical system-based model [33], steady-state thermochemical analysis [15,17], controller stability analysis [19], expert interviews [1,8] — authors arrive at a wide range of flexibility parameters that encompass different assumptions and concerns. A list of the specific flexibility parameters used by these authors are provided in Table 3. In this work, we investigate the full range of ramping and turndown flexibility but, we focus in particular on two cases: inflexible and best available technology (BAT). We use the flexibility parameters from [1] ($f_R = 0.2$ and $f_T = 0.4$) to represent the BAT case although they are conservative compared to some analyses in Table 3.

Beyond what is physically possible with flexible ammonia synthesis, there are additional design concerns when adapting an ammonia reactor loop designed for steady-state to flexible operation. Among these concerns are increased catalyst degradation in the reactor beds [7], mechanical stress from thermal cycling of reactors, and safety near unstable operating points [19,34]. Fatigue-based degradation models of batteries [35] and electrolyzers [36] in RE settings may provide a starting point for modeling degradation behaviors in the HBR [37]. Quantifying the impacts of thermal cycling and catalyst degradation will provide valuable insight and should be addressed in future techno-economic studies. However, it is out of the scope of this study and we do not include these effects in our analysis.

4.2. RE resource case study in Texas and Iowa

The wind and solar resources at any given location have a significant impact on the system design and resulting cost of ammonia. A brief comparison of some sites in Texas and Iowa with notable resource characteristics is presented in Table 4. A more comprehensive investigation of the effect of resource characteristics will be key in advancing the understanding of flexible green ammonia production but is left for future work.

Using the WTK [24] and NSRDB [25] data, we examine four candidate locations in Iowa and Texas each for the parameter sweep as detailed in Table 4. The cases are: Case 1. highest wind capacity factor (“Wind CF”), Case 2. highest solar capacity factor (“PV CF”), Case 3. highest complementarity of wind and solar, and Case 4. similar hybrid capacity factor and similar variability. We simulate an inflexible system

and BAT flexible system at each location.

Texas generally has better renewable resources than Iowa, allowing for greater energy production and higher overall ammonia production, as shown in the fifth row of Table 4. Apart from the PV capacity factor site (Case 2.), Texas has lower storage requirements than Iowa and lower LCOA. Although it is not a comprehensive analysis, these four cases clearly indicate that Texas is a superior location for producing green ammonia.

We choose Case 4., which emphasizes similarity in hybrid capacity factor and seasonal variability for a more in-depth comparison in Section 5. We choose this case not to demonstrate the absolute lowest possible LCOA but rather to show the potential for flexibility to enhance other aspects of system design.

4.3. Flexibility parameter sweep

Using Case 4. from Table 4, we sweep f_R and f_T from inflexible to fully flexible, optimizing the demand profile and computing the hydrogen storage requirements for each pair of parameters. The results are plotted in Fig. 5.

In both locations, the hydrogen storage capacity is far more sensitive to f_T than it is to f_R . The contours in Fig. 5 are nearly flat with respect to f_R except for at very low flexibility cases when $f_R < 0.001$. This result aligns with the conclusions of [8,9,11,14], which find ramping flexibility constraints to have minimal impact on the optimal system design. On the other hand, there is a clear gradient in storage capacity with respect to f_T in Fig. 5, indicating that turndown flexibility is one of the key factors behind storage requirements.

Similar to the results of [9,12], we find a decreasing sensitivity of the storage requirement to f_T as f_T increases. The majority of the storage requirement can be removed with $f_T = 0.2$ and although the storage continues to decrease with higher f_T , the benefit diminishes rapidly. This effect may be explained by the timescale of the RE variability that the system can accommodate for a given f_T . If the seasonal variability of the generation exceeds the HBR operating range, then the storage will need to discharge for months at a time to supplement the generation. If instead, the HBR is flexible enough to follow the seasonal variability trends, then the storage is only needed for short duration services, which can be provided with smaller storage capacity.

4.4. Costs

The costs for the generation subsystem are calculated within HOPP [27]. The wind and solar subsystem costs come from the NREL Annual Technology Baseline [38] and the PEM electrolyzer costs are calculated using the cost model from Singlitico et al. [39] and are shown in Table 5. For further details regarding the cost calculations for the generation subsystem, the reader is encouraged to reference the HOPP documentation [27].

The costs for the storage subsystem are also calculated within HOPP. Due to economies of scale there is no single value for the CapEx and OpEx of either the hydrogen storage or battery storage. The battery storage cost model is implemented in HOPP based off the NREL System Advisor Model (SAM) tool [40]. The hydrogen storage cost model is also implemented within HOPP using pipe-based and cavern-based hydrogen storage cost models from Papadias et al. [23].

The cost calculations for the end-use subsystem follow the method in [21]. Capital Expenditures (CapEx) are calculated based off the size of the component S , a cost constant K , and an exponential factor n according to Eq. (11). The Operating Expenditures (OpEx) are assumed to be a constant 5% of CapEx per year [21].

$$CapEx = K S^n \quad (11)$$

The specific parameters used to calculate end-use subsystem costs are provided in Table 6.

Table 4

Comparison of candidate locations in Texas and Iowa with significant wind or solar resource characteristics: Case 1. highest wind capacity factor, Case 2. highest solar capacity factor, Case 3. highest complementarity of wind and solar, and Case 4. similar hybrid capacity factor and similar variability. Where relevant, data is shown with the inflexible value followed by a slash then the BAT value (inflexible/BAT). We use Case 4. for detailed analysis in the remainder of this study.

	1. Wind CF		2. PV CF		3. Complimentarity		4. CF+Variability	
	IA	TX	IA	TX	IA	TX	IA	TX
Wind CF	0.37	0.43	0.33	0.32	0.24	0.26	0.37	0.33
PV CF	0.26	0.29	0.26	0.35	0.25	0.27	0.26	0.29
LCOE [¢/kWh]	3.75	3.25	4.01	3.75	5.05	4.63	3.75	3.92
AEP [TWh]	2.50	2.86	2.35	2.58	1.90	2.08	2.50	2.42
Ammonia [t/yr]	245 340	280 700	230 840	253 770	186 950	204 210	245 340	237 860
H ₂ storage [t]	2401/614	2067/357	2575/392	3787/647	2713/616	2183/607	2401/614	2100/328
HBR Rating [t/h]	28/37	32/41	26/35	28/38	21/30	23/32	28/37	27/36
LCOA [\$/t]	635/514	536/436	687/529	711/501	855/668	738/611	635/514	631/508

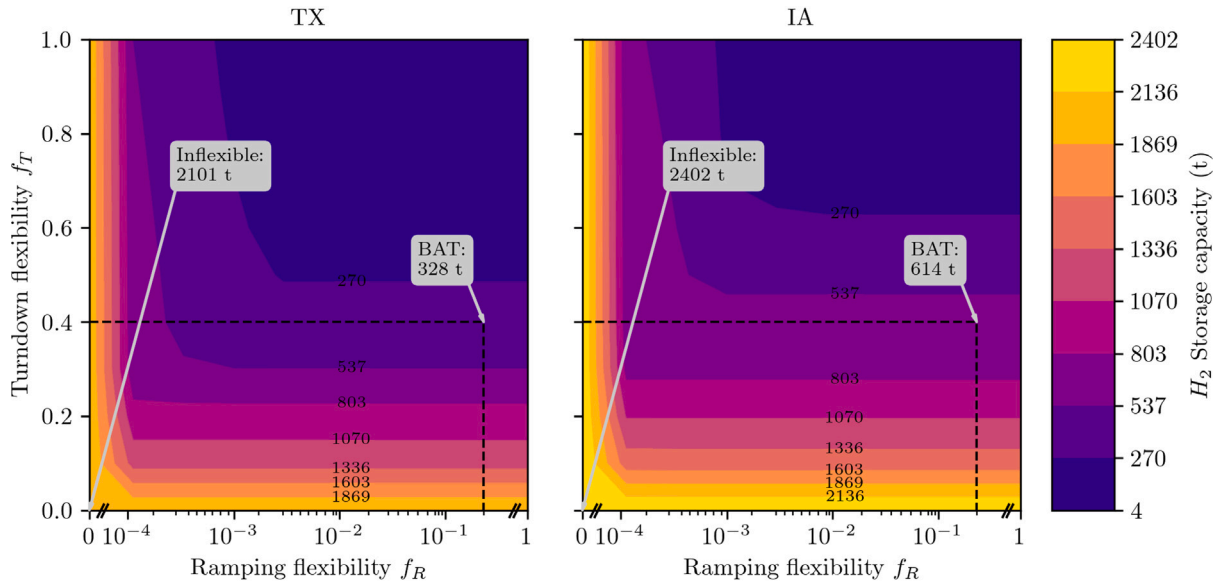


Fig. 5. Surface plot of hydrogen storage requirement for a sweep of ramping and turndown flexibilities in Texas and Iowa. The Texas BAT flexible case gives a 84.34% reduction in storage and the Iowa BAT flexible case gives a 74.45% reduction in storage. Texas has a steeper gradient with respect to turndown flexibility than IA, which means it has a better resource with lower variability. Note the ramping flexibility is plotted on a logarithmic scale, which has been modified to include 0 and 1 out of scale.

Table 5

Capex and Opex for wind, solar, and electrolyzer components [38,39].

Technology	CapEx		OpEx	
Wind farm	1530.31	\$/kW	60.90	\$/kW/yr
Solar farm	1146.68	\$/kW	21.24	\$/kW/yr
PEM electrolyzer	514.20	\$/kW	12.60	\$/kW/yr

Table 6

CapEx cost scaling parameters for the HBR and ASU [21].

Component	K	n	Size units
HBR	3.4×10^6	0.50	t/day NH ₃
ASU	9.2×10^5	0.49	t/day NH ₃

The LCOA is calculated as

$$LCOA = \frac{CapEx_{tot} + OpEx_{tot} \cdot L}{L \cdot \sum_{k=0}^{8760} \dot{m}_{NH_3,k} \Delta t}, \quad (12)$$

where $\dot{m}_{NH_3,k}$ is the hourly ammonia production, $CapEx_{tot}$ and $OpEx_{tot}$ are the total system costs, and L is the system lifetime, which is set to 30 years. Eq. (12) is implemented in Step 5 of Fig. 2.

5. Discussion

5.1. LCOA analysis

For the LCOA analysis, ramping flexibility is set to a constant value of $f_R = 0.2$, and we compare pipe storage and salt cavern storage in Iowa and Texas. Fig. 6 shows the LCOA contributions from each component in the off-grid ammonia system as a function of f_T , location, and storage type. As f_T increases, two trends emerge: the cost

contribution from the storage components (H₂ and battery) decreases and the cost contribution from the end-use components (HBR and ASU) increases. As f_T increases, the end-use becomes increasingly oversized to absorb a wider range of peaks and valleys in the generation signal, which accounts for the increase in end-use cost contribution to LCOA. The storage components decrease with flexibility, since the end-use can directly absorb more of the generation variability.

Fig. 5 shows a large reduction in hydrogen storage capacity for a relatively small increase in turndown flexibility from $f_T = 0$ to $f_T = 0.4$, which is reflected in the cost of the storage components in Fig. 6. This trend is more evident in Fig. 6a. and 6c. due to the higher cost of pipe storage compared to cavern storage. In both storage technologies, the majority of the cost savings from storage reduction come when f_T increases from 0 to 0.4, after which the cost savings are less significant, which aligns with the findings of [9,12].

The LCOA values for the inflexible and BAT cases are annotated in Fig. 6. The inflexible case has high storage capacity requirements resulting in a high LCOA for pipe storage. However, the flexible case

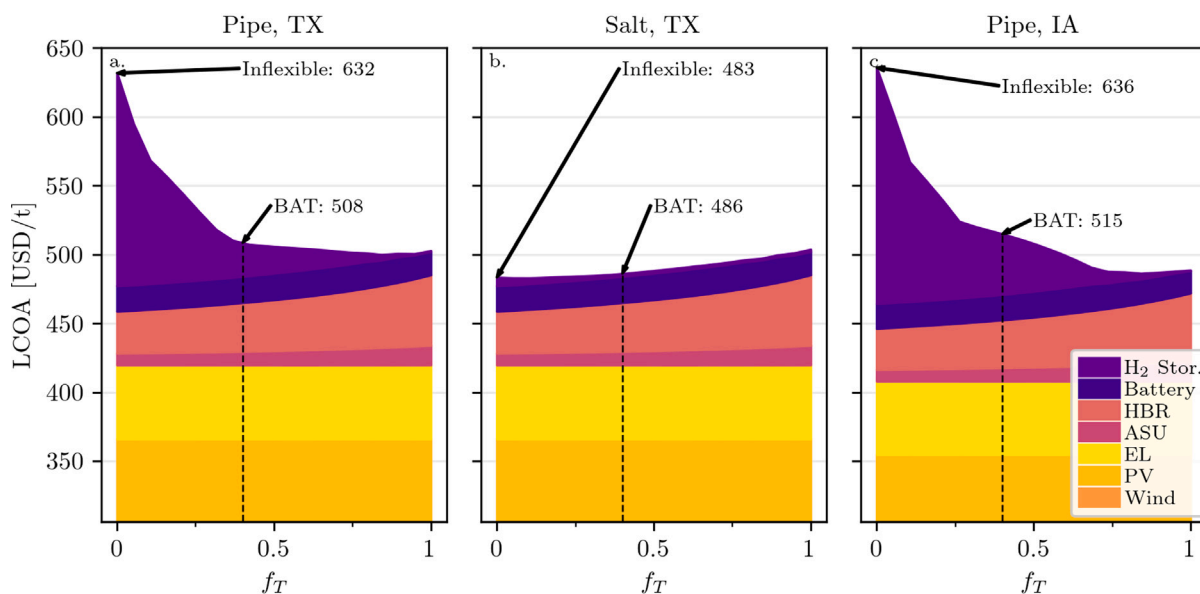


Fig. 6. LCOA sweep of $f_T \in [0, 1]$ with $f_R = 0.2$ for the Texas and Iowa locations showing the cost contributions from all system components. The vertical dashed line indicates a turndown flexibility of $f_T = 0.4$ corresponding to the BAT. Subplots a. and c. show the LCOA reduction attainable through HBR flexibility when using pipe-based hydrogen storage (21.8% reduction in TX and 21.0% reduction in IA). Subplot b. shows the LCOA attainable with salt cavern hydrogen storage in Texas only because Iowa has no natural salt deposits. The cost savings from replacing pipe-based storage with salt cavern storage outweigh those from flexibility alone; however in locations without salt deposits, HBR flexibility can offer a comparable LCOA reduction.

representing BAT reduces the LCOA with pipe storage to a point where it is competitive with an inflexible system using salt cavern storage. While salt cavern storage is usually more cost-effective at industrial scale, the flexible system with pipe storage can be made cost effective without being geographically constrained. This locational versatility allows the plant designer to pursue alternative goals such as better renewable resources or proximity to ammonia customers to avoid transportation costs.

Our findings align well with several of the techno-economic studies listed in Table 1. In Fig. 6, the LCOA decreases by 21.8% for the Texas site and 21.0% for the Iowa site when comparing BAT to inflexible. Salmon et al. [12] show roughly a 12% reduction in LCOA for the same two flexibility cases although their calculated LCOAs are slightly higher than ours. Smith et al. [13] find a reduction in LCOA as high as 53% for one location comparing inflexible to flexible HBR cases albeit with greater flexibility than we assume. Campion et al. [9] find LCOA reductions of 15%–19% in the three locations they investigated. Although there is little consensus among the studies in Table 1 about the LCOA attainable with flexibility, our results are generally consistent with other authors and are comparable with [8,12,14].

5.2. U.S. hybrid and ammonia plant locations

Our detailed analysis thus far considered only two sites. To place these in context, we also run our LCOA analysis on two additional sets (332 in total) of potential locations in the U.S., shown in Fig. 7. The first set of locations is the currently operational U.S. hybrid plants from [41], which is chosen to represent locations with attractive RE resource. The second set of locations is the set of U.S. ammonia plants from [42], which is chosen to show locations with access to existing ammonia infrastructure.

The Texas and Iowa case study locations are also plotted in Fig. 7. In both sets of locations, the LCOA spans a wide range values but lowest is similar between the two and is comparable with our Texas and Iowa case study locations. Fig. 7 further demonstrates the value of HBR flexibility showing that a significantly higher number locations are capable of reaching a given LCOA target with flexible operation than without.

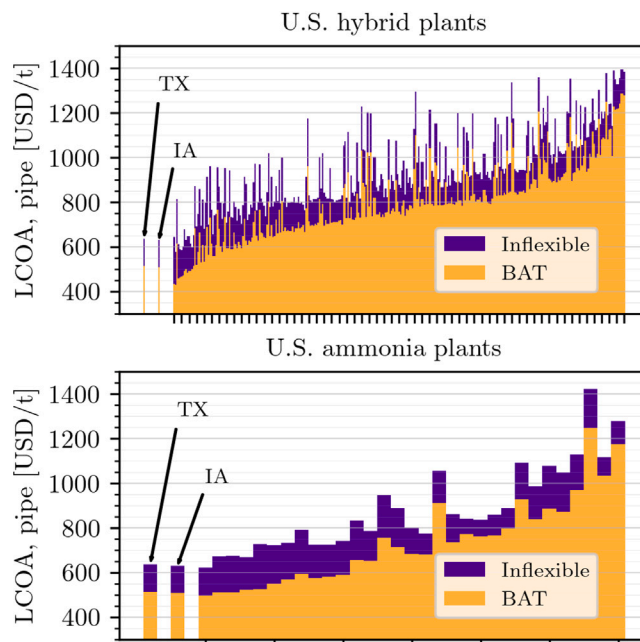


Fig. 7. LCOA for inflexible and BAT-flexible plants using pipe-based hydrogen storage evaluated at the locations of U.S. hybrid power plants [41] (top subplot) and U.S. ammonia plants [42] (bottom subplot). The locations are sorted from left to right in descending order by annual ammonia production. The Texas and Iowa results from our case study are plotted as separate bars on the left.

5.3. Impact of starting date

Although the starting date of the representative year optimization has no impact on the results and may be arbitrarily chosen as discussed in Section 3.4, the absolute starting date when the plant first goes online may be an important decision. The time of year that the plant starts producing ammonia is an important consideration in the design of the system due to the seasonal variability of the wind and solar

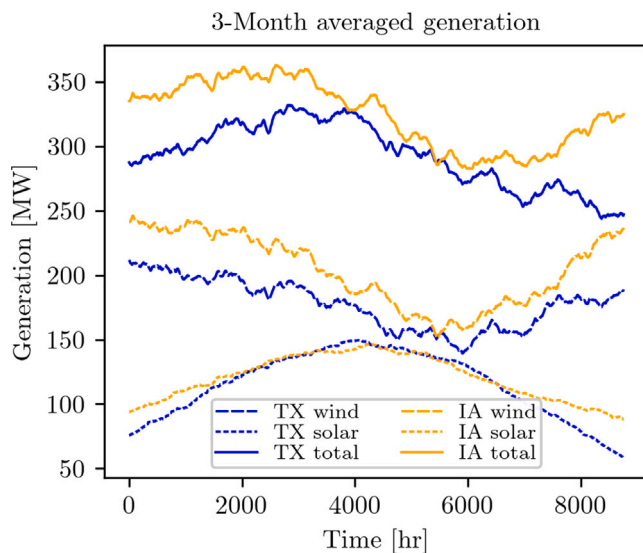


Fig. 8. Wind, solar, and combined generation profiles for Iowa and Texas using 2012 data [24,25]. The hourly generation profiles from WTK and NSRDB are filtered with a 3-month moving average filter to highlight the seasonal variation for each location. The range of the filtered data plotted as the standard deviation is used to quantify the seasonal variability, which is 88.1 MW in Texas and 77.0 MW in Iowa.

generation shown in Fig. 8. Unless the storage is pre-charged by other means, it is necessary to start the ammonia production when there is higher than average generation so that the storage subsystem can charge to support the plant for the rest of the year when there is lower than average generation. The best time to start production depends on both RE resource and the wind/solar mix for each individual scenario.

6. Conclusion

In this paper, we analyze the potential for flexibility in the HBR to decrease the hydrogen storage requirement and thus the LCOA of green ammonia production. We found that with reactor flexibility achievable with existing technology, the hydrogen storage capacity can be reduced by up to 84%, which in turn lowers the LCOA by 22% compared to an inflexible ammonia reactor. Our analysis shows that turndown flexibility is more impactful than ramping flexibility, particularly for managing seasonal RE variability. This suggests that implementing relatively small increase in reactor turndown flexibility can make green ammonia production more economically viable in locations without access to low-cost salt cavern hydrogen storage. By reducing the dependence on large-scale storage, more expensive pipe-based hydrogen storage can be used, which opens new opportunities for green ammonia plants to be built in locations with access to existing ammonia infrastructure or agriculture marketplaces.

Future work should investigate the effects of RE resource characteristics with a deeper look at wind/solar sizing and location, and improve the ammonia reactor sizing methodology with an optimization-based approach. In conclusion, enabling the flexible operation of ammonia reactors presents an economically viable pathway towards decarbonizing ammonia production using renewable energy generation.

CRedit authorship contribution statement

Zachary Tully: Writing – review & editing, Writing – original draft, Visualization, Software, Methodology, Investigation, Formal analysis, Conceptualization. **Jennifer King:** Writing – review & editing, Supervision, Methodology, Funding acquisition, Conceptualization. **Kathryn Johnson:** Writing – review & editing, Supervision, Methodology, Conceptualization.

Declaration of competing interest

The authors declare that they have no known competing financial interests or personal relationships that could have appeared to influence the work reported in this paper.

Acknowledgments

This work was authored in part by the National Renewable Energy Laboratory, operated by Alliance for Sustainable Energy, LLC, for the U.S. Department of Energy (DOE) under contract No. DE-AC36-08GO28308. Funding provided by U.S. Department of Energy Office of Energy Efficiency and Renewable Energy, Wind Energy Technologies Office, and Hydrogen and Fuel Cell Technologies Office. The views expressed in the article do not necessarily represent the views of the DOE or the U.S. Government. The U.S. Government retains and the publisher, by accepting the article for publication, acknowledges that the U.S. Government retains a nonexclusive, paid-up, irrevocable, worldwide license to publish or reproduce the published form of this work, or allow others to do so, for U.S. Government purposes.

Additional thanks go to Dylan Wald, Masha Koleva, and Kaitlin Brunik for their feedback and help with preparing this manuscript.

References

- [1] IEA. Ammonia technology roadmap. Paris: IEA; 2021. <http://dx.doi.org/10.1787/f6daa4a0-en>.
- [2] Chehade G, Dincer I. Progress in green ammonia production as potential carbon-free fuel. *Fuel* 2021;299:120845. <http://dx.doi.org/10.1016/j.fuel.2021.120845>.
- [3] Fasihi M, Weiss R, Savolainen J, Breyer C. Global potential of green ammonia based on hybrid PV-wind power plants. *Appl Energy* 2021;294:116170. <http://dx.doi.org/10.1016/j.apenergy.2020.116170>.
- [4] Wang M, Khan MA, Mohsin I, Wicks J, Ip AH, Sumon KZ, et al. Can sustainable ammonia synthesis pathways compete with fossil-fuel based Haber–Bosch processes? *Energy Environ Sci* 2021;14(5):2535–48. <http://dx.doi.org/10.1039/D0EE03808C>.
- [5] Kakavand A, Sayadi S, Tsatsaronis G, Behbahania A. Techno-economic assessment of green hydrogen and ammonia production from wind and solar energy in Iran. *Int J Hyd Egy* 2023;48(38):14170–91. <http://dx.doi.org/10.1016/j.ijhydene.2022.12.285>.
- [6] Cameli F, Kourou A, Rosa V, Delikonstantis E, Galvita V, Van Geem KM, et al. Conceptual process design and technoeconomic analysis of an e-ammonia plant: Green H₂ and cryogenic air separation coupled with Haber–Bosch process. *Int J Hyd Egy* 2024;49:1416–25. <http://dx.doi.org/10.1016/j.ijhydene.2023.10.020>.
- [7] Osman O, Sgouridis S, Sleptchenko A. Scaling the production of renewable ammonia: A techno-economic optimization applied in regions with high insolation. *J Clean Prod* 2020;271:121627. <http://dx.doi.org/10.1016/j.jclepro.2020.121627>.
- [8] Armijo J, Philibert C. Flexible production of green hydrogen and ammonia from variable solar and wind energy: Case study of Chile and Argentina. *Int J Hyd Egy* 2020;45(3):1541–58. <http://dx.doi.org/10.1016/j.ijhydene.2019.11.028>.
- [9] Campion N, Nami H, Swisher PR, Vang Hendriksen P, Münster M. Techno-economic assessment of green ammonia production with different wind and solar potentials. *Renew Sustain Energy Rev* 2023;173:113057. <http://dx.doi.org/10.1016/j.rser.2022.113057>.
- [10] Bouaboula H, Ouikhalfan M, Saadouni I, Chaouki J, Zaabout A, Belmabkhout Y. Addressing sustainable energy intermittence for green ammonia production. *Energy Rep* 2023;9:4507–17. <http://dx.doi.org/10.1016/j.egy.2023.03.093>.
- [11] Nayak-Luke RM, Bañares-Alcántara R. Techno-economic viability of islanded green ammonia as a carbon-free energy vector and as a substitute for conventional production. *Energy Environ Sci* 2020;13(9):2957–66. <http://dx.doi.org/10.1039/D0EE01707H>.
- [12] Salmon N, Bañares-Alcántara R. Impact of process flexibility and imperfect forecasting on the operation and design of Haber–Bosch green ammonia. *RSC Sustain* 2023;1(4):923–37. <http://dx.doi.org/10.1039/D3SU00067B>.
- [13] Smith C, Torrente-Murciano L. The importance of dynamic operation and renewable energy source on the economic feasibility of green ammonia. *Joule* 2024;8(1):157–74. <http://dx.doi.org/10.1016/j.joule.2023.12.002>.
- [14] Wang C, Walsh SDC, Longden T, Palmer G, Litalo I, Dargaville R. Optimising renewable generation configurations of off-grid green ammonia production systems considering Haber–Bosch flexibility. *Energy Convers Manage* 2023;280:116790. <http://dx.doi.org/10.1016/j.enconman.2023.116790>.
- [15] Cheema I, Krewer U. Operating envelope of Haber–Bosch process design for power-to-ammonia. *RSC Adv* 2018;8(61):34926–36. <http://dx.doi.org/10.1039/C8RA06821F>.

- [16] Cheema II, Krewer U. Optimisation of the autothermal NH₃ production process for power-to-ammonia. *Processes* 2020;8(1):38. <http://dx.doi.org/10.3390/pr8010038>.
- [17] Fahr S, Schiedeck M, Schwarzhuber J, Rehfeldt S, Peschel A, Klein H. Design and thermodynamic analysis of a large-scale ammonia reactor for increased load flexibility. *Chem Eng J* 2023;471:144612. <http://dx.doi.org/10.1016/j.cej.2023.144612>.
- [18] Deng W, Huang C, Li X, Zhang H, Dai Y. Dynamic simulation analysis and optimization of green ammonia production process under transition state. *Processes* 2022;10(10):2143. <http://dx.doi.org/10.3390/pr10102143>.
- [19] Rosbo JW, Ritschel TKS, Hørsholt S, Huusom JK, Jørgensen JB. Flexible operation, optimisation and stabilising control of a quench cooled ammonia reactor for power-to-ammonia. *Comput Chem Eng* 2023;176:108316. <http://dx.doi.org/10.1016/j.compchemeng.2023.108316>.
- [20] Sun Z, Zhang Y, Huang H, Luo Y, Lin L, Jiang L. Modeling and simulation of dynamic characteristics of a green ammonia synthesis system. *Energy Convers Manage* 2024;300:117893. <http://dx.doi.org/10.1016/j.enconman.2023.117893>.
- [21] Nayak-Luke R, Bañares-Alcántara R, Wilkinson I. “Green” ammonia: Impact of renewable energy intermittency on plant sizing and levelized cost of ammonia. *Ind Eng Chem Res* 2018;57(43):14607–16. <http://dx.doi.org/10.1021/acs.iecr.8b02447>.
- [22] Andersson J, Grönkvist S. Large-scale storage of hydrogen. *Int J Hyd Egy* 2019;44(23):11901–19. <http://dx.doi.org/10.1016/j.ijhydene.2019.03.063>.
- [23] Papadias DD, Ahluwalia RK. Bulk storage of hydrogen. *Int J Hyd Egy* 2021;46(70):34527–41. <http://dx.doi.org/10.1016/j.ijhydene.2021.08.028>.
- [24] Draxl C, Clifton A, Hodge B-M, McCaa J. The wind integration national dataset (WIND) toolkit. *Appl Energy* 2015;151:355–66. <http://dx.doi.org/10.1016/j.apenergy.2015.03.121>.
- [25] Sengupta M, Xie Y, Lopez A, Habte A, Maclaurin G, Shelby J. The national solar radiation data base (NSRDB). *Renew Sustain Energy Rev* 2018;89:51–60. <http://dx.doi.org/10.1016/j.rser.2018.03.003>.
- [26] Lambe AB, Martins JRRA. Extensions to the design structure matrix for the description of multidisciplinary design, analysis, and optimization processes. *Struct Multidiscip Optim* 2012;46(2):273–84. <http://dx.doi.org/10.1007/s00158-012-0763-y>.
- [27] NREL. Hybrid optimization and performance platform. NREL; 2023, URL <https://github.com/NREL/HOPP>.
- [28] DOE. Technical Targets for Proton Exchange Membrane Electrolysis, energy. gov URL <https://www.energy.gov/eere/fuelcells/technical-targets-proton-exchange-membrane-electrolysis>.
- [29] DOE. National transmission needs study. Tech. rep, U.S. Department of Energy; 2023, URL <https://www.energy.gov/gdo/national-transmission-needs-study>.
- [30] Murphy C, Harrison-Atlas D, Grue N, Mosier T, Gallego-Calderon J, Elliott S. Complementarity of renewable energy-based hybrid systems. Tech. rep NREL/TP-6A20-81901, 1972008, MainId:82674, 2023, <http://dx.doi.org/10.2172/1972008>.
- [31] Smith C, Hill AK, Torrente-Murciano L. Current and future role of Haber-Bosch ammonia in a carbon-free energy landscape. *Energy Env Sci* 2020;13(2):331–44. <http://dx.doi.org/10.1039/C9EE02873K>.
- [32] Virtanen P, Gommers R, Oliphant TE, Haberland M, Reddy T, Cournapeau D, et al. SciPy 1.0: fundamental algorithms for scientific computing in Python. *Nat Methods* 2020;17(3):261–72. <http://dx.doi.org/10.1038/s41592-019-0686-2>.
- [33] Allman A, Daoutidis P. Optimal scheduling for wind-powered ammonia generation: Effects of key design parameters. *Ch. E. R. D.* 2018;131:5–15. <http://dx.doi.org/10.1016/j.cherd.2017.10.010>.
- [34] Morud JC, Skogestad S. Analysis of instability in an industrial ammonia reactor. *AIChE J* 1998;44(4):888–95. <http://dx.doi.org/10.1002/aic.690440414>.
- [35] Li Y, Vilathgamuwa M, Choi SS, Xiong B, Tang J, Su Y, et al. Design of minimum cost degradation-conscious lithium-ion battery energy storage system to achieve renewable power dispatchability. *Appl Energy* 2020;260:114282. <http://dx.doi.org/10.1016/j.apenergy.2019.114282>.
- [36] Alia SM, Stariha S, Borup RL. Electrolyzer durability at low catalyst loading and with dynamic operation. *J Electrochem Soc* 2019;166(15):F1164–72. <http://dx.doi.org/10.1149/2.0231915jes>.
- [37] Zagorowska M, Wu O, Ottewill JR, Reble M, Thornhill NF. A survey of models of degradation for control applications. *Annu Rev Control* 2020;50:150–73. <http://dx.doi.org/10.1016/j.arcontrol.2020.08.002>.
- [38] Akar S, Beiter P, Cole W, Feldman D, Kurup P, Lantz E, et al. 2020 annual technology baseline (ATB) cost and performance data for electricity generation technologies. National Renewable Energy Laboratory - Data (NREL-DATA), Golden, CO (United States); National Renewable Energy Laboratory (NREL), Golden, CO (United States); 2020, <http://dx.doi.org/10.7799/1644189>.
- [39] Singlitico A, Østergaard J, Chatzivasileiadis S. Onshore, offshore or in-turbine electrolysis? Techno-economic overview of alternative integration designs for green hydrogen production into Offshore Wind Power Hubs. *Renew Sustain Energy Transit* 2021;1:100005. <http://dx.doi.org/10.1016/j.rset.2021.100005>.
- [40] NREL. System advisor model. NREL; 2022, URL <https://sam.nrel.gov/>.
- [41] Gorman W, Rand J, Manderlink N, Cheyette A, Bolinger M, Seel J, et al. Hybrid power plants: Status of operating and proposed plants, 2024 edition | energy markets & policy. Lawrence Berkeley National Lab; 2024.
- [42] Statista. U.S. ammonia plant capacities 2022. 2024, Statista URL <https://www.statista.com/statistics/1266392/ammonia-plant-capacities-united-states/>.